PERGAMON

International Journal of Heat and Mass Transfer 43 (2000) 2313–2324

International Journal of HEAT and MASS TRANSFER

www.elsevier.com/locate/ijhmt

An experimental study of gas–liquid flow in a narrow conduit

Z.Y. Bao, D.F. Fletcher*, B.S. Haynes

Department of Chemical Engineering, University of Sydney, Sydney, NSW 2006, Australia

Received 20 April 1999; received in revised form 17 September 1999

Abstract

This paper reports an experimental study of non-boiling air–water flows in a narrow conduit (diameter 1.95 mm). Results are presented for pressure drop characteristics and for local heat transfer coefficients over a wide range of gas superficial velocity (0.1–50 m s^{-1}), liquid superficial velocity (0.08–0.5 m s^{-1}) and wall heat flux (3–58 kW m^{-2}). For a given liquid flow rate, the data exhibit sudden changes in pressure drop and, to a lesser extent, in heat transfer characteristics as the gas flow is increased. These events are believed to correspond to flow transitions, from bubbly, to intermittent slug, to annular flow. Overall, the pressure drops in these diabatic non-boiling two-phase flows can be estimated with good accuracy using correlations developed for adiabatic conditions. The heat transfer results are, on average, reasonably well described by the two-phase convective heat transfer components of flow-boiling correlations but there is considerable scatter in some cases.

Keywords: Non-boiling; Two phase; Air–water; Pressure drop; Heat transfer; Fine passage

1. Introduction

Compact heat exchangers have traditionally found wide application in the transport industry because of their attractive features, which include: high thermal effectiveness, small size, low weight and design flexibility. There is widespread interest in expanding the range of applications of compact heat exchangers to include phase change heat transfer for application in the process industry. It is therefore, necessary to have a good understanding of the characteristics of the flow and heat transfer in narrow conduits.

The frictional pressure drop and the heat transfer coefficient are the two most important parameters in heat exchanger design. Experimental data on two-phase flow heat transfer has been obtained by many workers and numerous correlations have been developed. Examples include those of: Lockhart–Martinelli [1], Baroczy [2], Chisholm [3], Beattie [4], Beattie and Whalley [5], Kopalinsky and Bryant [6] and Müller-Steinhagen and Heck [7] for pressure drop, and Chen [8], Bennet and Chen [9], Shah [10], Gungor and Winterton [11,12], Klimenko [13,14] Liu and Winterton [15], Kandlikar [16,17] and Steiner and Taborek [18] for heat transfer. However, most of these correlations are based on data obtained from relatively large diameter conduits and the predictions from these correlations show considerable variability. This is because of the large number of relatively poorly understood parameters upon which two-phase momentum and

* Corresponding author. Tel.: +61-2-9351-4147; fax: +61-2-9351-2854.

E-mail address: davidf@chem.eng.usyd.edu.au (D.F. Fletcher).

0017-9310/00/$ - see front matter
PII: S0017-9310(99)00297-5

Nomenclature

C_i^a	conductance between zone i and the environment (W K^{-1})
C_i^b	conductance between zone i and zone $i+1$ (W K^{-1})
C_p	heat capacity at constant pressure (J kg^{-1} K^{-1})
f	Fanning friction factor
G	mass flux (kg m^{-2} s^{-1})
H	enthalpy (J kg^{-1})
h	heat transfer coefficient (W m^{-2} K^{-1})
$\dot{m}$	mass flow rate (kg s^{-1})
P	pressure (N m^{-2})
Q	heat flow (W)
q	heat flux (W m^{-2})
Re	Reynolds number
T	temperature (K)
U_S	superficial velocity (m s^{-1})
x	quality

Greek symbol

λ	latent heat of vaporization (J kg^{-1})

Subscripts

f	fluid
G	gas
i	block number i
in	inlet value
L	liquid
loss	lost to surroundings
0	ambient value
out	outlet value
pred	predicted value
W	wall value

Superscript

^	block averaged value

heat transfer depend. This is especially true for flow in very narrow passages, where there is relatively little data and different physical phenomena may be of importance. Therefore, the objective of this work is to provide data on two-phase pressure drop and non-boiling heat transfer in fine passages. In this manner, a study of two-phase convective heat transfer can be made whilst avoiding the complexity of boiling heat transfer. This work provides a basis for future research in the area of two-phase flow heat transfer and heat exchanger design.

2. The experimental study

2.1. The experimental facility

The experimental facility used to determine pressure drop and heat transfer measurements for two-phase air–water flows as shown in Fig. 1. Most experiments were performed with the test section horizontal but the effect of vertical upward and downward flow were also examined. The gas and liquid flows were maintained using calibrated mass-flow controllers. The test section is an 870 mm length of straight copper tubing with an inner diameter of 1.95 mm and outer diameter 3.175 mm. The gas and liquid flows are mixed in a tee junction prior to the test section. The first 400 mm of the test section tube is unheated and serves to allow full hydrodynamic development of the flow ahead of the heated test section, of length 270 mm, which is in turn followed by a 200 mm long exit section. The entry, test and exit sections are all lagged with foam insulation to minimize the heat loss and the influence of the external environment.

The test section is divided into 10 separate heating zones, as shown in Fig. 2, with each zone being electrically heated via a band heater attached to the outside of a cylindrical copper block which surrounds the test section. In order to obtain good thermal contact between the tube and the blocks, the components are soldered together. The length and outside diameter of the blocks is 25 mm. Adjacent blocks are separated via a 2 mm thickness of insulation to minimize the interaction between adjacent blocks.

The interior temperature of each block is measured using a thermocouple embedded in the copper block, close to the tubing wall. The block temperature

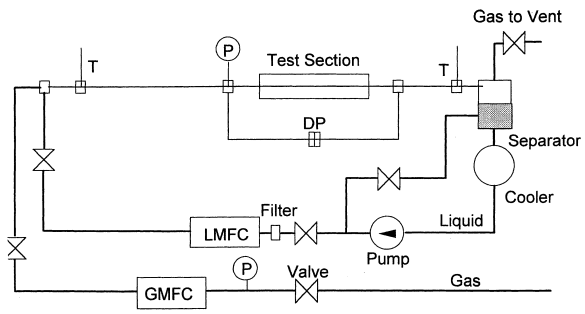

Fig. 1. A schematic of the experimental apparatus. (On the diagram DP = Differential Pressure transducer, LMFC = Liquid Mass Flow Controller, GMFC = Gas Mass Flow Controller.)

measurements are made differentially with respect to the entrance temperature of the fluid, with a minimum detectable temperature difference of 0.02 K. The outlet temperature is also measured using a thermocouple. Tests were conducted to check the radial temperature profiles in the copper blocks. It was confirmed that, over the range of experiments, the radial temperature variations are negligible and that the temperatures measured by the embedded thermocouples are equivalent to the wall temperatures of the tube.

All of the outputs of the thermocouples are acquired by a data logger (Datataker 100) and stored in a personal computer. Pressures and pressure drops across the test section are measured using appropriate transducers (Transinstruments 2000 and Motorola MPX2200/2010, respectively) at pressure taps located 65 mm upstream and 65 mm downstream of the test section. The flow is hydrodynamically developed prior to the upstream tap, so that the average pressure gradient across the test section is determined directly from these two measurements.

2.2. Calibration of the heating zone

The experimental apparatus was employed to obtain local values of the heat transfer rate for each of the 10 blocks. The heat transfer network model employed in the analysis of this section is shown in Fig. 3. The steady-state heat balance for each block is given by:

$$Q_1 = Q_{f1} + Q_{a1} + Q_{1,2} \tag{1}$$

$$Q_i = Q_{fi} + Q_{ai} + Q_{i,i-1} + Q_{i,i+1} \quad 2 \le i \le 9 \tag{2}$$

and

$$Q_{10} = Q_{f10} + Q_{a10} + Q_{10,9} \tag{3}$$

where Q_i is the heat input into block i, Q_{fi} is the heat transferred to the flow in zone i, Q_{ai} is the heat lost to the environment, and $Q_{i,j}$ is the inter-block heat flow between adjacent blocks i and j.

The resistance network may be calibrated as follows. If there is no fluid flow in the test section, the heat transferred to the fluid $Q_{fi} = 0$ and the sum of the heat lost to the environment and that transferred to adjacent zones must be equal to the input heat Q_i. It is also assumed that the thermal resistance between each heating zone and the surroundings, and between adjacent zones are independent of temperature and the direction of heat flow, which is justified because the major mechanism of heat transfer is thermal conduction. Therefore, the heat transfer rate can be expressed as:

$$Q_{ai} = C_i^a (T_i - T_0) \quad (i = 1, 2, 3, \ldots, 10) \tag{4}$$

$$Q_{i,i+1} = C_i^b (T_i - T_{i+1}) \quad (i = 1, 2, 3, \ldots, 9) \tag{5}$$

where C_i^a is the thermal conductance between zone i and the environment, T_0 is the ambient air temperature and C_i^b is the thermal conductance between zone i and zone $i+1$. These equations can be solved if the block temperatures are measured for two different heat inputs to yield values for the conductances C^a and C^b, i.e.

$$Q_1^{(k)} = C_1^a \left(T_1^{(k)} - T_0^{(k)} \right) + C_1^b \left(T_1^{(k)} - T_2^{(k)} \right) \tag{6}$$

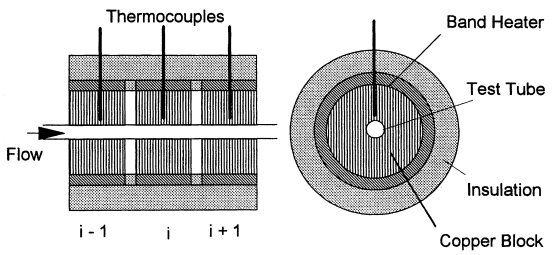

Fig. 2. A schematic of the heating zone arrangement, showing the copper block construction.

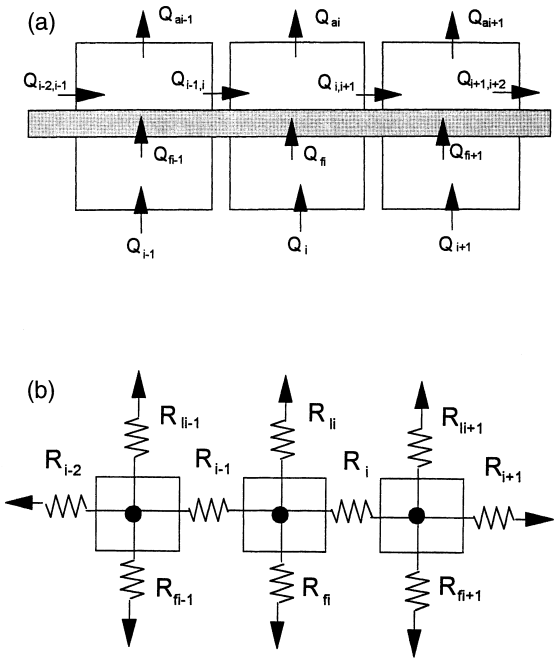

Fig. 3. A schematic of (a) the heat flows, and (b) the heat transfer resistances in the heating zones.

Table 1
Values of the conductances to the surroundings and between adjacent zones

Zone number	Mean C^a (W K^{-1})	Standard deviation of C^a (%)	Mean C^b (W K^{-1})	Standard deviation of C^b (%)
1	0.02900	6.79	0.351	8.29
2	0.00901	12.9	0.369	9.97
3	0.00826	17.4	0.353	6.98
4	0.00910	5.97	0.345	7.49
5	0.00864	6.47	0.370	6.24
6	0.01062	7.70	0.306	4.89
7	0.00836	8.80	0.320	6.45
8	0.01001	6.60	0.330	6.70
9	0.00866	11.6	0.344	9.87
10	0.02724	6.34	–	–

$$Q_i^{(k)} = C_i^a\left(T_1^{(k)} - T_0^{(k)}\right) + C_{i-1}^b\left(T_i^{(k)} - T_{i-1}^{(k)}\right) + C_i^b\left(T_i^{(k)} - T_{i+1}^{(k)}\right) \quad (i = 2, 3, \ldots, 9) \tag{7}$$

$$Q_{10}^{(k)} = C_{10}^a\left(T_{10}^{(k)} - T_0^{(k)}\right) + C_9^b\left(T_{10}^{(k)} - T_9^{(k)}\right) \tag{8}$$

for $k = 1, 2$. In order to determine the C_i^a and C_i^b from the above equations the values of the $T_i^{(k)}$ and $T_0^{(k)}$ and the heat input Q_i must be known. The values of the Q_i are calculated from the resistance of each band heater, R_i, and the input voltage, V, (both measured using a multimeter) via $Q_i = V^2/R_i$.

A number (12 runs) of calibration experiments were performed under no flow conditions, using a wide range of heating schemes and block temperatures. A total of nine estimates of each conductance was obtained, giving the results summarized in Table 1. The inter-block conductances (C^b) are typically 30 times higher than the ambient loss conductances (C^a), except for the end blocks which, as expected, have substantially higher loss conductances. The standard deviation of the inter-block conductances is always less than 10% and for the loss conductances it is less than 20%. These uncertainties have very little effect on the heat transfer analysis for cases with fluid flow because more than 70% (and, typically, 90%) of the heat input to a given block is transferred to the fluid in that block rather than lost to other blocks or to the surroundings.

2.3. Tests using single phase flows

The system was tested using single phase flows of air or liquid to verify its performance. The measured Fanning friction factor was compared with that predicted for laminar flow and that predicted by the Colebrook–White correlation for turbulent flow in smooth circular tubes. As shown in Fig. 4, there is good agreement between the experimental and predicted friction factor, f_{exp} and f_{pred}, for both laminar flow ($Re < 2000$) and turbulent flow ($Re > 2000$).

The heating system was also tested for single phase liquid flow heat transfer measurements. The total heat loss from the system was calculated from these temperatures and the conductances C_i^a found earlier, using

$$Q_{loss} = \sum_{i=1}^{10} C_i^a (T_i - T_0) \tag{9}$$

At steady-state, the overall system heat balance gives

$$\sum_{i=1}^{10} Q_{fi} = \dot{m} C_p (T_{f\,out} - T_{f\,in}) = \sum_{i=1}^{10} Q_i - Q_{loss} \tag{10}$$

where $\dot{m}$ is the fluid mass flowrate, C_p is the fluid heat capacity, and $T_{f\,in}$ and $T_{f\,out}$ are the inlet and outlet temperatures. Analysis showed that the total heat loss to the environment was less than 5% of the heater

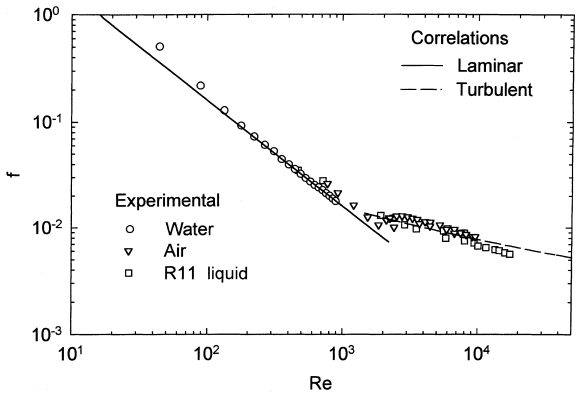

Fig. 4. Comparison of the experimentally determined friction factor with predictions from standard correlations for single phase flow.

power and that the inter-block heat transfer was also less than 5% under all circumstances, except for the end blocks.

The bulk mean fluid temperature in each zone was determined from the integral heat balance from the entry of the test section to the mid-point of the zone via

$$\dot{m}\Delta\hat{H}_i = \dot{m}\hat{C}_p(T_{fi} - T_{f\,in}) = \sum_{j=1}^{i-1} Q_j + Q_i/2 \tag{11}$$

Knowing the wall temperature, T_{Wi}, and the fluid temperature, T_{fi} (calculated from Eq. (11)), as well as the wall heat flux, q_i, it is therefore, possible to determine pseudo-local heat transfer coefficients in a thermally developing flow via

$$h_i = \frac{q_i}{(T_{Wi} - T_{fi})} \tag{12}$$

The comparison of experimentally determined heat transfer coefficients in single phase turbulent flow of liquid Freon R11 with those predicted by the Gnielinski correlation [19] for smooth circular tubes is shown in Fig. 5. The data show excellent agreement with the correlation over the Reynolds number range of 3000–20,000 studied here.

2.4. Accuracy of the method

Eqs. (11) and (12) provide the basis for estimation of the propagation of errors in these experiments. The electrical heat output from the heaters is determined to better than 1%, with the bulk of this output going into the fluid in the block zone in which the heater is located. Uncertainty in the inter-block heat transfer and losses amounts conservatively to 10% of these quantities, or no more than 3% of the total heat input from the heaters. With an uncertainty in the mass flowrate of less than 2%, the temperature rise of the fluid from its inlet value (Eq. (11)) is estimated to be uncertain by no more than 5%.

The bulk mean temperature difference at a given block is determined from the difference between the measured wall temperature excess (measured differentially with respect to the fluid inlet temperature) and the calculated temperature rise of the fluid. The former quantity is established to within 0.02 K, while the latter is, as described above, accurate to within 5% or 0.05 K for a nominal 1 K per block temperature rise. This leads to a maximum uncertainty of 7% in the local temperature difference between the wall and the fluid.

Allowing for uncertainties in the local heat flux

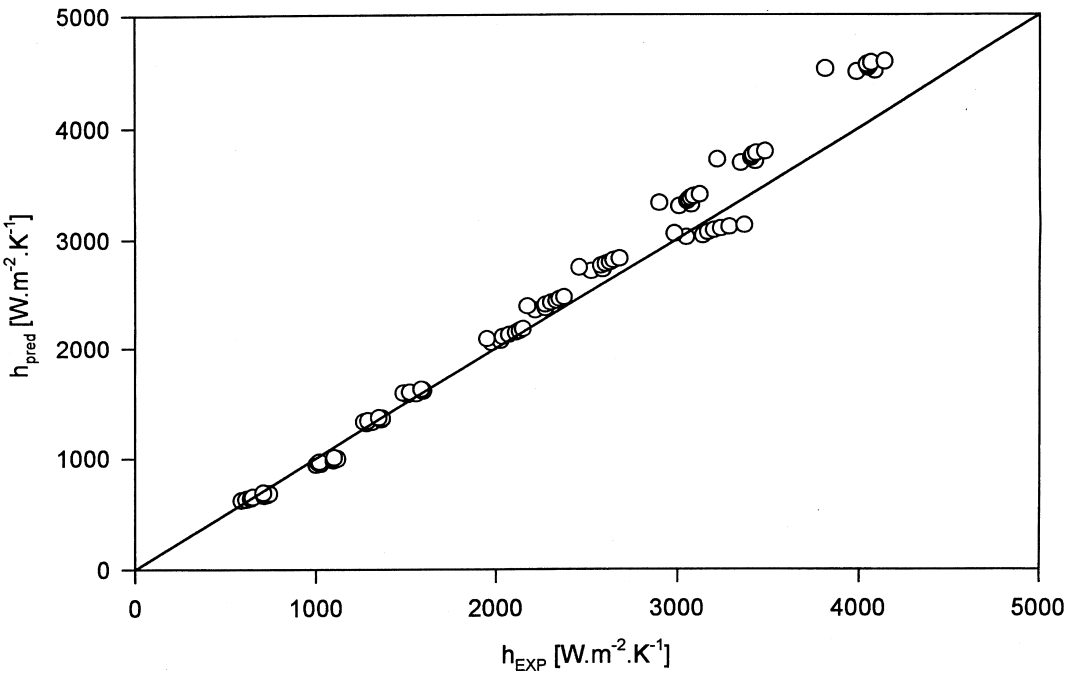

Fig. 5. A comparison of experimentally determined local heat transfer coefficients for the single phase turbulent flow of liquid Freon R11 with predictions from the Gnielinski [19] correlation.

(±3%, as described above) leads to the conclusion that the local heat transfer coefficient averaged over each block is accurate to within 10%. This conclusion is borne out by the comparisons of measurement and predictions for single-phase flows described in Section 2.3 and shown in Fig. 5.

3. Results and discussion

3.1. Pressure drop

Typical relationships between the experimental frictional pressure drop and superficial gas velocity, for a constant liquid velocity, are shown in Fig. 6. In general, the frictional pressure gradient increases with increasing gas and liquid superficial velocities. However, at a constant liquid velocity, four different regions may be identified in this figure. In the region of low velocity, the frictional pressure drop increases with increasing gas velocity, but then approaches a local maximum. For the lower superficial velocities ($U_{SL} = 0.11$–0.21 m s^{-1}, corresponding to $Re_L =$ 220–410) the peak occurs at $U_{SG} \approx 0.4$–0.6 m s^{-1} ($Re_G = 50$–60) but for $U_{SL} = 0.41$ m s^{-1} ($Re_L = 794$) the peak occurs at $U_{SG} \approx 1$ m s^{-1} ($Re_G = 150$). Beyond this peak, the frictional pressure drop decreases slightly with increasing gas velocity until a minimum is reached. This is referred to as the second region. The third region corresponds to moderate superficial gas velocities. In this region the pressure drop again increases with increasing superficial gas velocity, until an inflection point is reached at $U_{SG} \approx 6$–8 m s^{-1}. In the fourth region, at higher gas velocities still, the pressure gradient increases more steeply with increasing gas velocity.

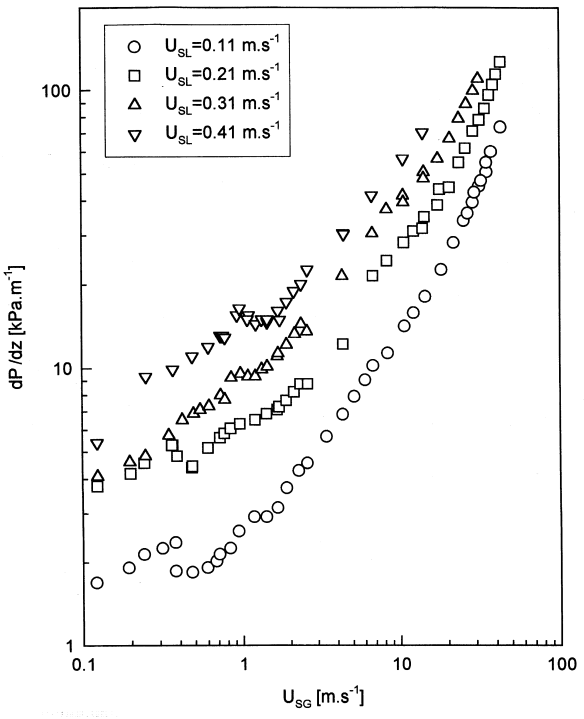

Fig. 6. A plot of the frictional pressure gradient in a horizontal adiabatic air–water flow in a 1.95 mm diameter copper tube at constant superficial velocity as a function of superficial gas velocity. The exit pressure is 1.2 bar.

Similar phenomena have been observed with air–water flow in rectangular channels by Wambsganss et al. [20], as is shown in their Fig. 7 of experimental pressure gradient against quality, for flow at a fixed mass flux of 500 kg m^{-2} s^{-1}. Although the inflection points were not mentioned by Wambsganss et al. [20], their existence can be seen clearly on their graphs. Similar phenomena were also documented for flow in capillary tubes by Ozawa et al. [21]. According to Ozawa et al., the intermediate zone of decreasing pressure gradients is the region over which there is transition of the flow from capillary bubbly flow to slug flow. This is consistent with the results of flow pattern studies for each of three rectangular geometries studied by Wambsganss et al. [20,22,23].

It was not possible to identify the flow patterns directly in these studies, but comparison with the studies of flow patterns in glass tubes [24] reveals that the flow in the first region is mainly bubbly flow, while the second region corresponds to the transition from bubbly to intermittent flow. Region three is identified with intermittent flow (elongated bubble or slug flow) and in the fourth region the flow is mostly annular. The critical velocities at which the pressure gradients reach a local maximum are very close to those at which transition from bubbly flow to intermittent flow (elongated bubble or slug flow) occurs, whilst the inflection points are close to the transition region from slug to annular flow. From Fig. 6 it is evident that there is no sudden change in the pressure drop when the transition from slug to annular flow occurs.

In addition, it was found that in the first region the fluctuations in the system pressure and in the total pressure drop across the test section were very small, whereas in the second region these fluctuations were very large. In region three the fluctuations remained large but decreased gradually towards the inflection point. In the last region, the amplitude of the fluctuations was very small but their frequency was very high. These observations are consistent with the results of flow pattern observations. Flow pattern transitions have previously been associated with void fraction [25]. The void

Table 2
The range of parameters considered in the heat transfer tests

Parameter	Range
Diameter, d (mm)	1.95
System pressure, P (kPa)	110–260
Gas mass flux, G_G (kg m^{-2} s^{-1})	0.7–106
Liquid mass flux, G_L (kg m^{-2} s^{-1})	78–492
Gas quality, x	0.0012–0.57
Superficial gas velocity, U_{SG} (m s^{-1})	0.1–50
Superficial liquid velocity, U_{SL} (m s^{-1})	0.08–0.5
Gas Reynolds number, Re_G	70–11,110
Liquid Reynolds number, Re_L	150–1400
Lockhart–Martinelli parameter, X	0.1–8.2
Fluid temperature, T_f (°C)	20–54
Wall temperature, T_W (°C)	22–68
Heat flux, q (kW m^{-2})	3–58
Heat transfer coefficient, h (kW m^{-2} K^{-1})	0.9–24

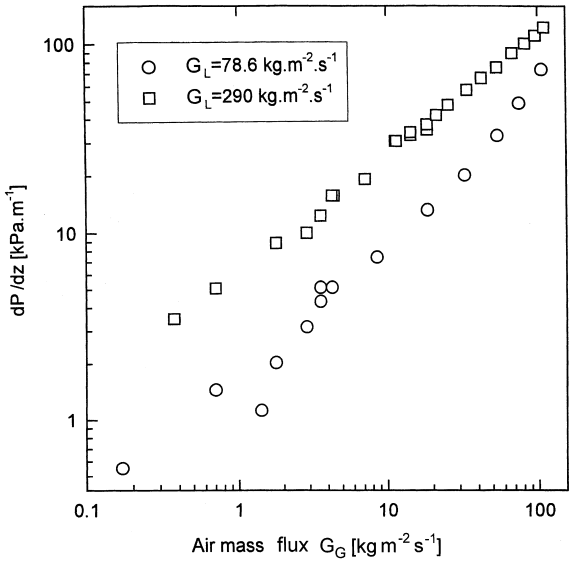

Fig. 7. A plot of the frictional pressure drop against gas mass flux, G_G, for an air–water flow with heat transfer.

fractions were calculated using the Lockhart–Martinelli correlation and this showed that the characteristic inflections in the pressure drop curves occurred in the region where the void fraction, $\epsilon_G \sim 0.7$–0.8, which is close to the value of 0.76, the critical void fraction for slug to annular flow transition suggested by Barnea [25], based on a spontaneous blockage criterion. Wambsganss et al. [23] have also studied regime transition. They have identified simi-

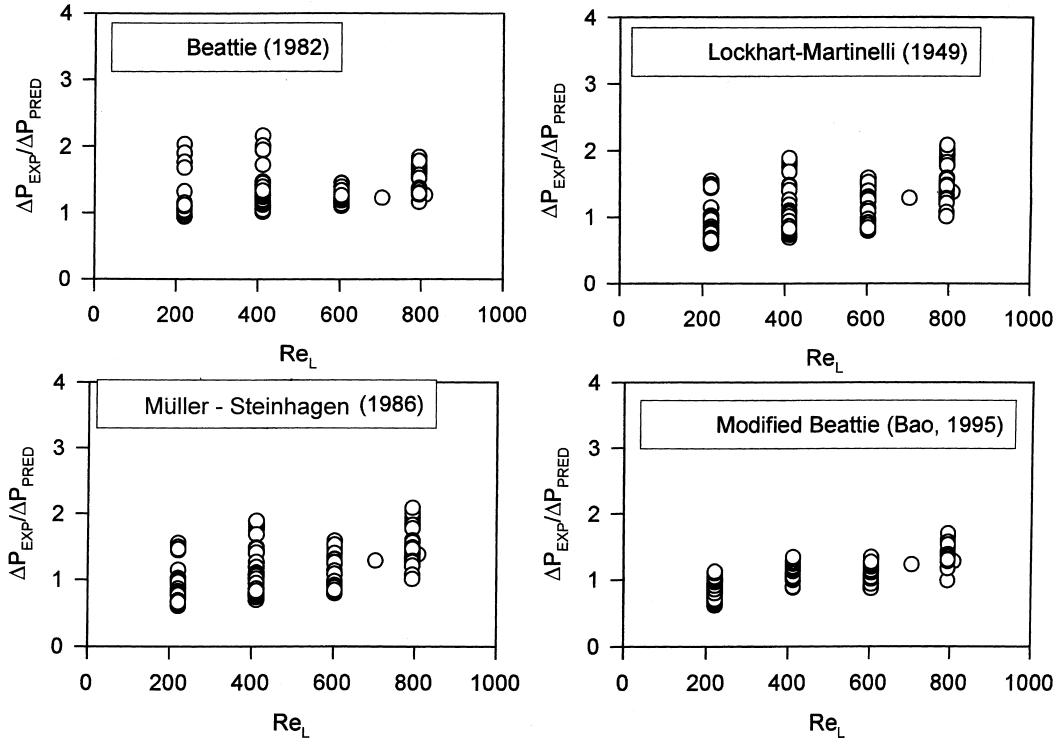

Fig. 8. Comparison of the experimentally determined pressure drop for adiabatic two-phase flow against the predictions of various correlations.

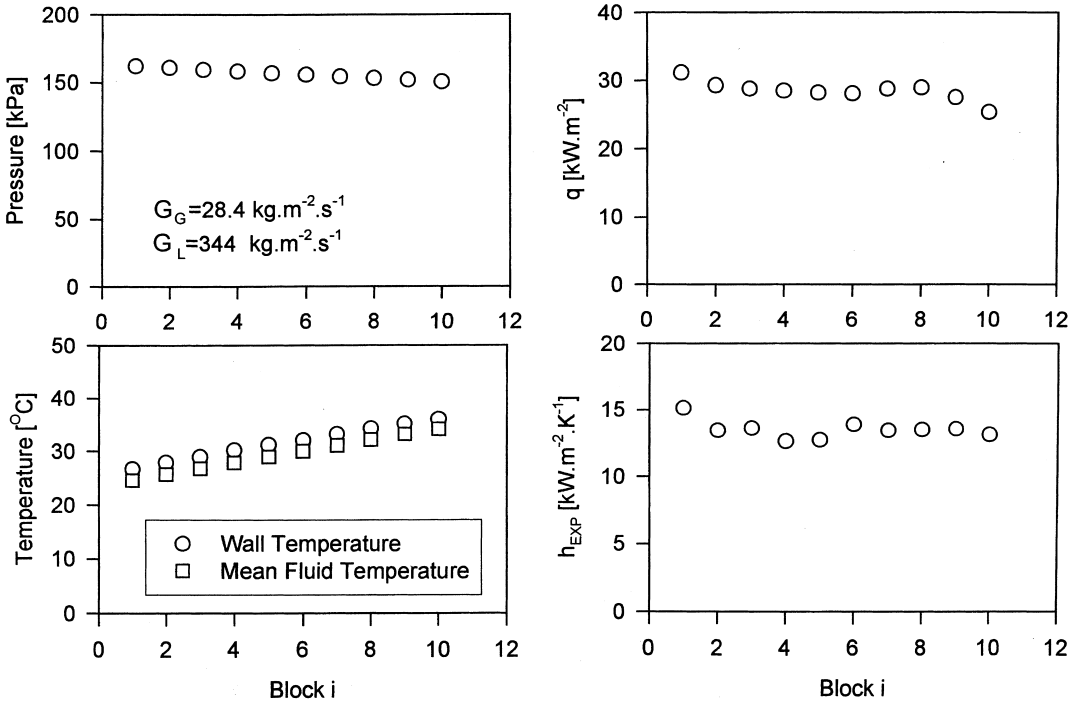

Fig. 9. A typical set of experimental data for pressure, section mean wall and fluid temperature, heat flux and heat transfer coefficient in individual heating sections for air–water horizontal flow.

lar regimes to those reported here, again based on changes of slope in RMS pressure drop against mass quality plots.

For the case of two-phase flow with heat transfer, the temperature of both the gas and liquid phases may be different at different locations in the channel. Therefore, the fluid properties vary along the channel. In order to determine the temperature of the mixture, the test section was divided into 12 subsections, according to the heating arrangement, i.e. the inlet section, the 10 heated sections and the outlet region. It was assumed that a uniform temperature is achieved within each subsection and that the fluid properties for each section are determined from the bulk temperature of the fluids. The total predicted frictional pressure drop is then the sum of those predicted for each subsection.

The range of experimental parameters for the non-boiling heat transfer experiments presented here are given in Table 2. The experimental measurements indicate that the air–water two-phase flows with non-boiling heat transfer are very similar to adiabatic two-phase flows. An example of this is shown in Fig. 7, where the experimental frictional pressure drop is plotted against the gas mass flux G_G, which is based on the gas phase flowrate and the mean bulk temperature in the test section. The curve for $G_L = 78.6$ kg m^{-2} s^{-1} reveals a sharp local maximum in the frictional pressure drop at low gas velocity and an inflection region a higher gas velocity. These features are consistent with those of adiabatic flows. For the $G_L =$ 290 kg m^{-2} s^{-1} case, the sharp decrease and the inflection point are less distinct.

The pressure drop predicted using the methods of Beattie [4], Lockhart–Martinelli [1], modified Müller-Steinhagen and Heck [7] and modified Beattie [26] are shown in Fig. 8. A detailed description of the correlations is given in Ref. [26] and the references therein. Although some of the experimental data are outside the range of validity of some of the correlations, they all give reasonable predictions over most of the liquid Reynolds number range. However, they generally fail to predict the local maximum in the pressure drop or the point of inflection.

The Lockhart–Martinelli correlation provides satisfactory predictions but has a tendency to underpredict the pressure drop. This is worst around the gas transition Reynolds number. Uncertainties in the value of the gas phase Reynolds number at which this transition occurs are thought to be the reason for this discrepancy. The modified Müller-Steinhagen and Heck correlation performs very well for the range tested, which is consistent with observations for adiabatic air–liquid flows with a superficial liquid Reynolds number

greater than 100. The Beattie correlation is valid only for turbulent flow and underpredicts the pressure drop for laminar two-phase flow. The predictions from the modified Beattie correlation are the closest to the measured data and exhibit the lowest scatter.

3.2. Heat transfer

For the case with heat transfer, the heat transfer coefficient is defined as in Eq. (12), with the values of q and T_W being determined experimentally. For air–water two-phase flows the fluid temperature, T_f, is defined as the bulk temperature for the mixture at equilibrium. The heat capacity of the mixture is calculated using

$$C_p = xC_{pG} + (1-x)C_{pL} \tag{13}$$

where x is the quality. There is a slight complication in this case compared with single phase flow, in that as heat is transferred to the water some evaporation occurs. It is readily shown that in this case the outlet temperature from heating section i is given by

$$T_{out,\,i} = T_{in,\,i} + \frac{Q_i - \Delta m_L \lambda}{\dot{m} C_{p,\,i}} \tag{14}$$

where Δm_L is the mass of water evaporated, which can be calculated from the vapour partial pressure, and λ is the enthalpy of vaporisation. The mean fluid temperature is then simply the arithmetic average of $T_{in,\,i}$ and $T_{out,\,i}$.

The outlet pressure, P_{out}, is calculated using the inlet pressure and the total pressure drop across the section, via

$$P_{out} = P_{in} + \Delta P_{pred} \tag{15}$$

In order to calculate the total pressure drop the Lockhart–Martinelli correlation was used to determine the void fraction and the modified Beattie correlation was used to predict the frictional pressure drop because these were found to be the best available correlations [26]. The mean pressure in any section was assumed to be the arithmetic average of the inlet and outlet values. As the fluid properties, the mean temperature and the mean pressure are inter-dependent, an iterative procedure was employed for each section to obtain a self-consistent mean temperature and pressure.

A total of 70 experimental runs were performed, yielding 700 data points for air–water flows. Of these: 58 were for horizontal flow, nine were for vertical flow and three were for downward flow. As expected, there was no significant effect of orientation as the gravitational component of the pressure drop is small compared with the frictional part. The ranges of parameters considered are given in Table 2.

A set of typical results for the mean pressure, the mean wall and fluid temperatures, the heat flux and the heat transfer coefficient are given as a function of heating section in Fig. 9 for a horizontal air–water flow. The figure shows that apart from the first two and the last two blocks the heat flux is almost constant. These differences are caused by end-block heat transfer to the surroundings. Despite these slight differences in the heat flux, the heat transfer coefficient is almost constant, except near the inlet. This effect occurs over a wide range of heat fluxes at constant mass flux and quality. In order to eliminate entrance effects, the data from the first two sections are not used in the subsequent analysis.

The measured heat transfer coefficients for the air–water system are always higher than would be expected for the corresponding single phase liquid flow, so that the addition of air can be considered to have an enhancing effect. This observation is consistent with the work of Chu and Jones [27] and Shah [28] for air–water flows. This presumably arises from the increased liquid velocity caused by the presence of the gas phase

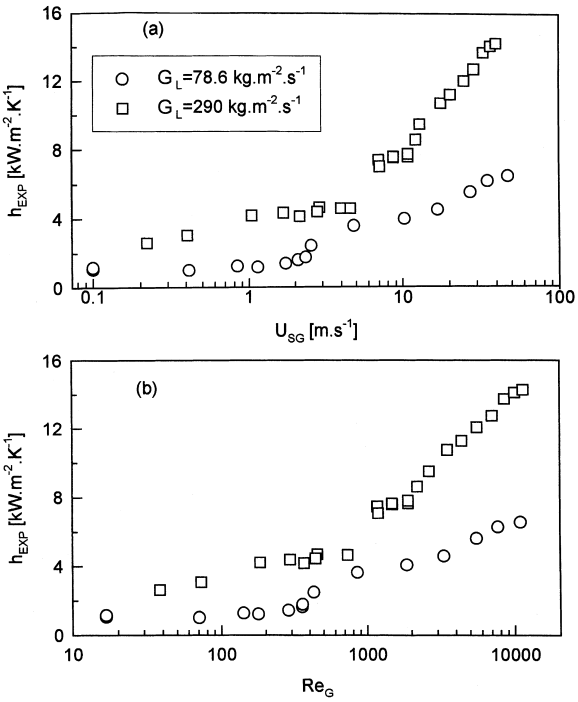

Fig. 10. A plot of the experimentally determined heat transfer coefficient as a function of the superficial gas velocity and the gas Reynolds number. The liquid mass fluxes are 78.6 and 290 kg m^{-2} s^{-1}, the heat fluxes are 20 and 33 kW m^{-2} and the pressure ranges from 140 to 200 kPa.

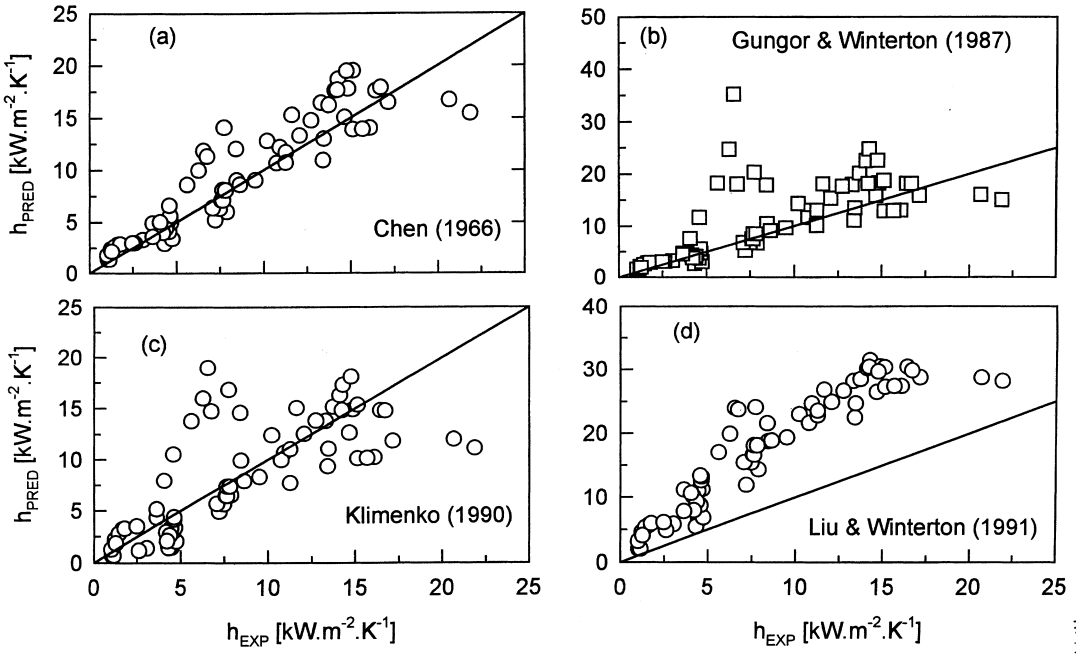

Fig. 11. A plot of the experimental heat transfer coefficients against those predicted by various correlations. The experimental data were collected at heating section 7.

and from higher turbulence intensities due to the relative motion between the phases.

Fig. 10 shows the experimental heat transfer coefficients for horizontal flows with: (a) a liquid mass flux of 78.6 kg m^{-2} s^{-1} and a heat flux of 20 kW m^{-2}, and (b) a liquid mass flux of 290 kg m^{-2} s^{-1} and heat flux of 33 kW m^{-2} plotted against the gas superficial velocity and plotted against the gas phase Reynolds number at heating section 7. As expected, the heat transfer coefficient increases with increasing liquid mass flux and increasing gas superficial velocity or Reynolds number. The data show a sharp increase in the heat transfer coefficient at a gas velocity of about 3 m s^{-1} ($Re_G \approx 600$) for the case of $G_L = 78.6$ kg m^{-2} s^{-1} and a gas superficial velocity of 5.5 m s^{-1} for the case of $G_L = 290$ kg m^{-2} s^{-1}. This is most likely caused by a change in flow regime. The measured frictional pressure drop for the same runs was presented in Fig. 7. Comparison of these figures shows that the location of the sudden jump in heat transfer coefficient corresponds to the inflection points in the curves for experimental pressure drop.

In Fig. 11, the experimental data are compared with predictions of selected correlations [8,12,15,14] assuming that the boiling term of these correlations was zero. Most of these correlations suggest that the convective component of heat transfer of two-phase flows can be correlated by multiplying the single phase liquid heat transfer coefficient, h_L, by an enhancement factor. Generally, h_L is predicted by the Dittus–Boelter equation for the liquid flow ($h = 0.023 Re_L^{0.8} Pr_L^{0.4} k_L/d$) which is applicable for $Re_L > 10{,}000$ and is certainly not applicable for $Re_L < 2000$. It is therefore, surprising that, although $Re_L < 2000$ in the present experiments, the predictions of all of the correlations are consistent with the measurements. This is attributable to the fact that the two-phase nature of the flow leads to transition to turbulence at much lower Reynolds numbers than in single phase flow.

As shown in Fig. 11, the Chen correlation [8] provides a good average prediction over the entire parameter range studied, albeit with some scatter. In this correlation, the enhancement factor was presented graphically and was fitted by Collier [29] as a function of the Lockhart–Martinelli parameter for turbulent–turbulent flow, X_{tt}. In the present work, however, the flows are not always in this regime and it is X, rather than X_{tt} which has been used in Chen's correlation, a change which led to some improvement in the fit to the data. The Gungor and Winterton [12] correlation was applied with the boiling number set to zero, and although the comparison is more scattered, a good average prediction is again obtained. The convective component of the Klimenko correlation [14] shows considerable scatter but is reasonable on average. Finally, the correlation of Liu and Winterton [15] con-

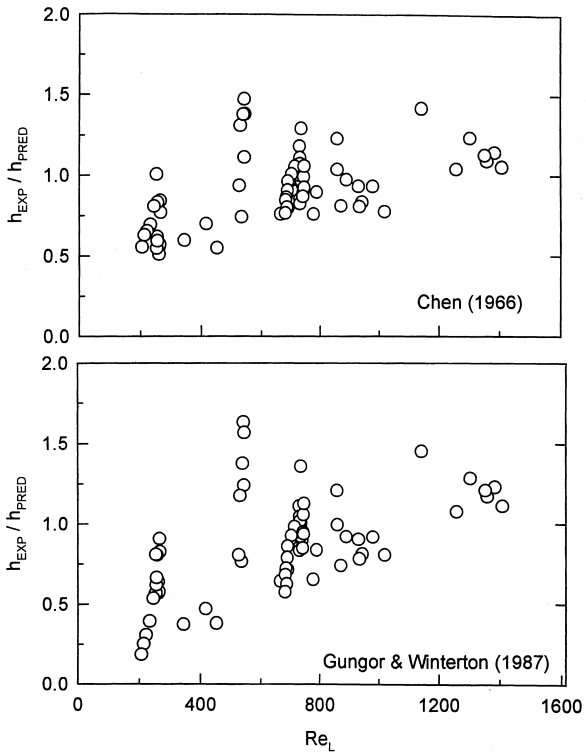

Fig. 12. A plot of the ratio of the experimentally determined heat transfer coefficients divided by the predicted values from the Chen [8] and Gungor and Winterton [12] correlations as a function of the liquid phase Reynolds number. The experimental data were collected at heating section 7.

siderably overpredicts the measurements but has a small scatter.

Fig. 12 shows a plot of the ratio of the experimental heat transfer coefficient divided by the predicted values of Chen [8] and Gungor and Winterton [12] versus liquid Reynolds number. It can be seen that both methods provide reasonable predictions for $Re_L > 500$, but that both overpredict the heat transfer coefficient at lower values of Re_L. Neither correlation predicts the sharp jump in the magnitude of the heat transfer coefficient with increasing U_{SG} at a constant U_{SL}, which is believed to be caused by a flow regime transition. This almost certainly contributes to the scatter in the comparison between the measured and predicted heat transfer coefficient data.

4. Conclusions

This paper contains detailed data on pressure drop and heat transfer for two-phase non-boiling flows in narrow conduits. The nature of the experimental setup means that local heat transfer rates can be determined. The data show very clearly that the pressure drop and heat transfer are very flow regime dependent. There is however little difference as far as pressure drop is concerned between adiabatic flows and those with heat transfer.

Existing heat transfer correlations, on average, do a reasonable job but there is the possibility of making significant errors if they are used outside the range investigated here. In boiling/condensing flows the effect of phase transition complicates further the regime transition effects. Whilst the convective component of heat transfer is well predicted by existing convective flow correlations, the enhancement due to phase change is more difficult to include.

Acknowledgements

Financial support for this work has been provided in part by Heatric Ltd.

References

[1] R.W. Lockhart, R.C. Martinelli, Proposed correlation of data for isothermal two-phase, two-component flow in pipes, Chemical Engineering Progress 45 (1949) 39–48.
[2] C.J. Baroczy, A systematic correlation for two-phase pressure drop, Chemical Engineering Progress Symposium Series 62 (1966) 232–249.
[3] D. Chisholm, Pressure gradients due to friction during the flow of evaporating two-phase mixtures in smooth tubes and channels, International Journal of Heat and Mass Transfer 16 (1973) 347–358.
[4] D.R.H. Beattie, A note on the calculation of two-phase pressure losses, Nuclear Engineering and Design 25 (1973) 395–402.
[5] D.R.H. Beattie, P.B. Whalley, A simple two-phase frictional pressure drop calculation method, International Journal of Multiphase Flow 8 (1982) 83–87.
[6] E.M. Kopalinsky, R.A.A. Bryant, Friction coefficients for bubbly two-phase flow in horizontal pipes, AIChE Journal 2 (1976) 82–86.
[7] H. Müller-Steinhagen, K. Heck, A simple friction pressure drop correlation for two-phase flow in pipes, Chemical Engineering Process 20 (1986) 297–308.
[8] J.C. Chen, Correlation for boiling heat transfer to saturated fluids in convective flow, I & EC Process Design and Development 5 (1966) 322–329.
[9] D.L. Bennet, J.C. Chen, Forced convective boiling in vertical tubes for saturated pure components and binary mixtures, AIChE Journal 26 (1980) 454–461.
[10] M.M. Shah, Prediction of heat transfer during boiling of cryogenic fluids flowing in tubes, Cryogenics 5 (1984) 231–236.
[11] K.E. Gungor, R.H.S. Winterton, A general correlation

for flow boiling in tubes and annuli, International Journal of Heat and Mass Transfer 29 (1986) 351–358.
[12] K.E. Gungor, R.H.S. Winterton, Simplified general correlation for saturated flow boiling and comparisons of correlations with data, Chemical Engineering Research and Design 65 (1987) 148–156.
[13] V.V. Klimenko, A generalised correlation for two-phase forced flow heat transfer, International Journal of Heat and Mass Transfer 31 (1988) 541–552.
[14] V.V. Klimenko, A generalised correlation for two-phase forced flow heat transfer — second assessment, International Journal of Heat and Mass Transfer 33 (1990) 2073–2088.
[15] Z. Liu, R.H.S. Winterton, A general correlation for saturated and subcooled flow boiling in tubes and annuli based on a nucleate pool boiling equation, International Journal of Heat and Mass Transfer 34 (1991) 2759–2766.
[16] S.G. Kandlikar, A general correlation for saturated two-phase flow boiling heat transfer inside horizontal and vertical tubes, ASME Journal of Heat Transfer 112 (1990) 219–228.
[17] S.G. Kandlikar, Development of a flow boiling map for subcooled and saturated flow boiling of different fluids inside circular tubes, ASME Journal of Heat Transfer 113 (1991) 190–200.
[18] D. Steiner, J. Taborek, Flow boiling heat transfer in vertical tubes correlated by an asymptotic model, Heat Transfer Engineering 13 (1992) 43–69.
[19] V. Gnielinski, New equations for heat and mass transfer in turbulent pipe and channel flow, International Chemical Engineering 16 (1976) 359–368.
[20] M.W. Wambsganss, J.A. Jendrzejczyk, D.M. France, Two-phase flow patters and transitions in a small, horizontal, rectangular channel, International Journal of Multiphase Flow 17 (1991) 327–342.
[21] M. Ozawa, K. Akagawa, T. Salaguchi, T. Fujii, Oscillatory flow instabilities in air–water two-phase flow system, Bulletin of JSME 22 (1979) 1763–1770.
[22] M.W. Wambsganss, J.A. Jendrzejczyk, D.M. France, N.T. Obot, Frictional pressure gradients in two-phase flow in a small horizontal rectangular channel, Experimental Thermal and Fluid Science Journal 5 (1992) 40–56.
[23] M.W. Wambsganss, J.A. Jendrzejczyk, D.M. France, Determination and characteristics of the transition to two-phase slug flow in small horizontal channels, Transactions of ASME—Journal of Fluids Engineering 116 (1994) 140–146.
[24] Z.Y. Bao, Gas–liquid two-phase flow and heat transfer in fine passages. PhD thesis, Department of Chemical Engineering, The University of Sydney, 1995.
[25] D. Barnea, Transition from annular flow and from dispersed bubble flow — unified models for the whole range of pipe inclinations, International Journal of Multiphase Flow 12 (1986) 733–744.
[26] Z.Y. Bao, M.G. Bosnich, B.S. Haynes, Estimation of void fraction and pressure drop for two-phase flow in fine passages, Transactions of IChemE, Part A 72 (1994) 625–632.
[27] Y.-C. Chu, B.G. Jones, Convective heat transfer coefficient studies in upward and downward, vertical, two-phase, non-boiling flows, AIChE Symposium Series 76 (1980) 79–90.
[28] M.M. Shah, Generalised prediction of heat transfer during two component gas–liquid flow in tubes and other channels, AIChE Symposium Series 77 (1981) 140–151.
[29] J.G. Collier, Gas–liquid flow, in: Heat Exchanger Design Handbook, vol. 2, Hemisphere, Washington, DC, 1983 (Section 2.32).